

# Design of a Pressure Sensor to Monitor Teeth Grinding

Ibrahim M. Abdel-Motaleb<sup>1</sup>, Kamran Ravanasa<sup>1</sup>, and Karl-Johan Soderholm<sup>2</sup>

<sup>1</sup>Department of Electrical Engineering, Northern Illinois University, Dekalb, IL, USA

<sup>2</sup>Department of Restorative Dental Sciences, College of Dentistry, University of Florida, Gainesville, FL USA

\*Corresponding author: ibrahim@niu.edu

**Abstract:** Studying teeth grinding behavior and other oral conditions requires the ability to accurately measure the pressure on the teeth. Placing a sensor in the mouth requires small size devices with powering and measurement techniques that do not hinder the normal life of the patient. To meet these requirements, we designed, using COMSOL, a small, easy to read MEMS capacitive force sensor, with adjustable dynamic range and high sensitivity. The sensor is a capacitive sensor and can be read using commercial RFID tag. A small RFID tag, with 3 mm antenna coil, is integrated with the sensor. The sensor is then implanted inside a pontic or a crown. If a force is applied on the reconstructed tooth (the sensor), a related change in the sensor's capacitance takes place. Since the sensor's capacitance is added in parallel to the tag's original capacitor, the change in the tag's capacitor results in changing the resonance capacitance of the tag. This can be related to the applied force. Using digital signal processing techniques, the tag's readings can be measured with high accuracy.

**Keywords:** Pressure sensor, Tooth grinding, MEMS.

## 1. Introduction

Pressure is defined as force per unit area. In our case, pressure sensors are used as transducers generating an electrical signal.

Electromagnetic, optical and potentiometric pressure sensors are not suitable for our case because of size, biocompatibility and cost.

In miniature size pressure sensors, piezoelectric and piezoresistive sensors are widely used [1]. Temperature dependency is the main negative point for not using piezoresistive sensor [2]. Also, power consumption in these sensors is not as low as it is in capacitive sensors, where it is almost zero.

The capacitive pressure sensor is used because of biocompatibility, low power consumption, low

temperature sensitivity, high dynamic range, high pressure sensitivity and miniature size.

Normally a capacitive pressure sensor has a diaphragm for sensing the pressure and by increasing the diaphragm size, reducing diaphragm thickness and decreasing sensing gap, we achieve the high sensitivity of the sensor [3]. Also the geometry of the capacitor can be changed to adjust dynamic range and sensitivity. For energizing (power source) and wireless monitoring; adaptive RF powering and inductive coupling was used by Peng Cong [4]. This method is very popular and is used by others too.

The sensor designed in this project uses the same idea of inductive coupling, where it uses a commercial RFID chip [5] and replaces its antenna with a small coil (in  $\mu\text{H}$  range) [4]. By inductive coupling, the coil can be energized while the size of the RFID chip and the antenna is still smaller than  $10 \text{ mm}^2$ . For monitoring the pressure, the capacitive sensor is added to a resonance tank. Changes in resonance frequency make it then possible to measure the pressure. Also, in the energizing circuit, the power source and size are not critical, and an adaptive filter can be used to adjust the energizing frequency to new resonance frequencies in order to improve reliability and freedom in design.

## 2. Use of COMSOL Multiphysics

### 2.1 Design of Capacitive Pressure Sensor and Pressure Range

The pressure and capacitor dimensions relationship is given below. By choosing appropriate values, we can access to desired pressure range:

$$x = \frac{3(1 - \nu^2)}{16} \frac{\Delta p R^4}{E t^3}$$
$$x < t$$
$$\Delta p_{max} = \frac{16}{3(1 - \nu^2)} \frac{E t^3 d}{R^4}$$
$$F = (p)A = kx$$

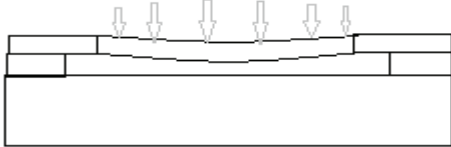


**Figure 1.** Deformation caused by applying force on Diaphragm

where R is the radius of diaphragm, E is the Young modulus of diaphragm=60 GPa, t is the thickness of diaphragm, v is the Poisson ratio of diaphragm=0.17, d is the gap=1 $\mu\text{m}$ . If t=1 $\mu\text{m}$ , R=100  $\mu\text{m}$ :

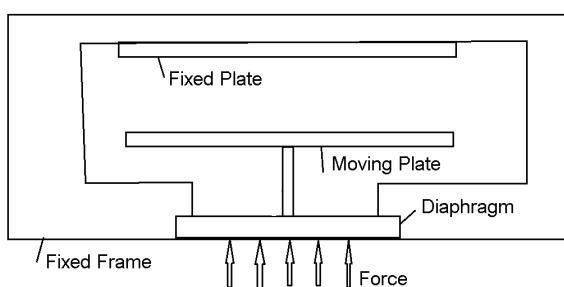
$$p_{max} = \frac{16 \times 60 \times 10^9 \times (10^{-6})^3 \times 1 \times 10^{-6}}{3(1 - 0.17^2)(100 \times 10^{-6})^4}$$

$$\Rightarrow p_{max} = 3.3 \text{ kPa}$$

With t=2 $\mu\text{m}$ , R=40  $\mu\text{m}$   $\Rightarrow p_{max} = 2.1 \text{ MPa}$   
This is good for our case.

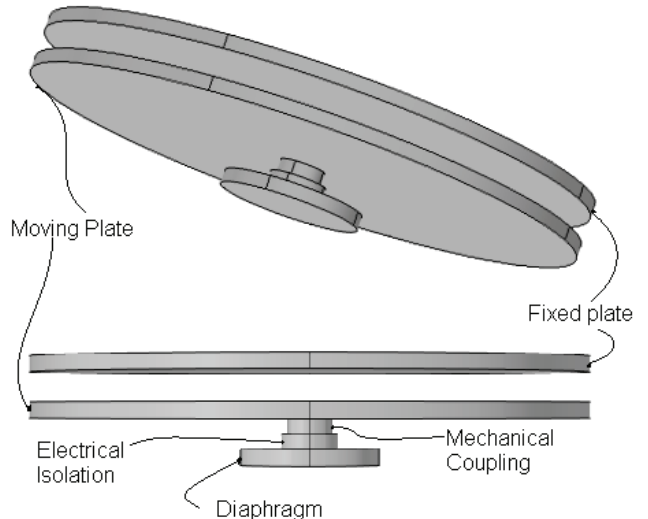
## 2.2 Sensor Design

Figure 2 shows the design of a capacitive pressure sensor. In this design, pressure sensing diaphragm is separated from the capacitor plates. The design includes three main parts; a diaphragm, a pair of capacitor plates (one fixed and one moving), and a mechanical coupling element. For higher dynamic range, the design is circular to maintain circular symmetry at edges. Using square diaphragm causes high stress at corners where the diaphragm is clamped. Square or rectangular diaphragms may lower dynamic range because of high stress points in the corners. Figure 2 shows how diaphragm clamped and how the fixed plate is fixed [3].



**Figure 2.** A schematic drawing of the sensor shows component locations

The moving plate, through a mechanical coupling element, is connected to the center of a diaphragm (and electrically isolated). The size of this element is small for having negligible effect on the diaphragm deflection.



**Figure 3.** A schematic drawing of the capacitive sensor. The pressure sensor diaphragm is coupled with moving plate of capacitor. Dimension ratios are changed for better visibility.

When the diaphragm deflects under pressure, the moving plate will deflect the same amount from the center and cause the capacitance change.

The capacitance sensitivity for circular pressure sensor is [3]

$$\frac{\Delta C}{P} = \frac{3(1 - \nu^2)R^4}{16ET^3} \frac{\epsilon_0 \epsilon_r A_{sense}}{g^2}$$

Where  $\Delta C$  is change in capacitance, P is the pressure difference across the diaphragm, R is the radius of diaphragm, T is the thickness of the diaphragm,  $A_{sense}$  is the area of moving plate and g is the sensing gap between moving plate and fixed plate. So by scaling the dimensions, we can achieve the proper dynamic range for pressure as it is calculated in the previous section.

In Figure 4 a FEM model simulation using COMSOL, is shown. It shows a deflected diaphragm under a pressure load.

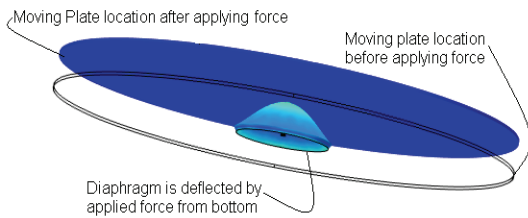


**Figure 4.** Simulation result with COMSOL. Pressure causes deformation of diaphragm and so it moves the moving plate

By electrically isolating the capacitor from the diaphragm, we are separating the capacitor from the environment.

Inside the tooth reconstruction, at least three sensors are needed for a stable crown or pontic. It will be shown later that when the force on each cone is less than 80 N the relationship between the sensor's capacitance and force is linear. Because of linearity the resulting capacitance represents the total force on the crown. In practice,  $4 \times 4 = 16$  cones (two is shown in Fig. 5) are used in a crown that transfers the force to sixteen sensors' diaphragms at sixteen contact cones. The space between the occlusal surface and the sensors is filled and glued with Neukasil RTV-23 material that is biocompatible and has a Young's modulus of 0.2 MPa, which is much less than Young's modulus of the polysilicon diaphragm, which Young's modulus is 60 GPa. Thus, the force on the occlusal surface is transferred to the sensors through the cones.

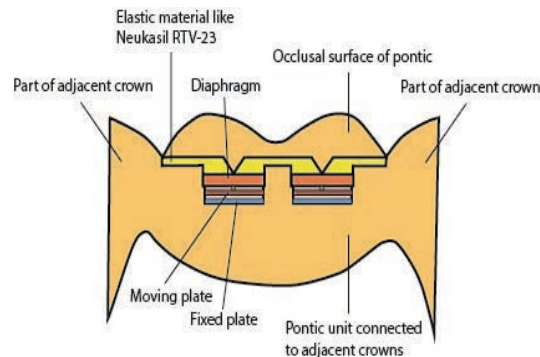


**Figure 5.** Sensors inside the pontic is shown in the xz plane. In the xy plane, there are four sensors located on a square vertices and the square center is located at the center of the pontic (not shown in the drawing). The low elastic modulus of the Neukasil RTV-23 layer I facilitates force transfer via the cones to the sensor diaphragms.

Using cones to transfer the force to the sensors causes the force to be applied to the diaphragms. Considering this point, the Figure 6 shows the COMSOL simulation model. The occlusal surface of the pontic is thick enough to use polysilicon.

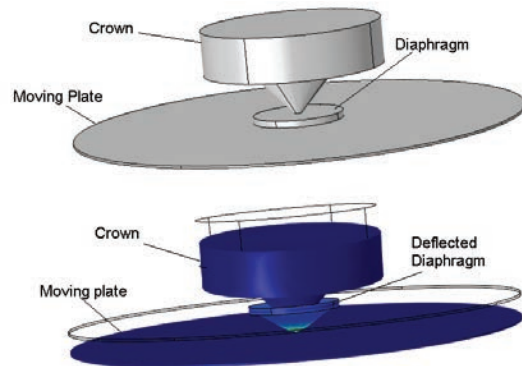


**Figure 6.** A schematic drawing of the capacitive sensor including part of occlusal surface. The top drawing shows the sensor before applying force and the bottom drawing shows it after applying the force. The diaphragm deflection was generated by COMSOL simulation.

For achieving linearity between capacitance change and force, 20 sensors are placed inside the pontic. Final design of one sensor is shown in Figure 7. Dimensions are: diaphragm thickness: 9  $\mu\text{m}$ , Radius: 4  $\mu\text{m}$ ; Cone thickness: 10  $\mu\text{m}$ , radius: 18  $\mu\text{m}$ . Pontic is much thicker and bigger than these dimensions.

The displacement of a moving plate versus force is generated by a COMSOL simulation and shown in Figure 8.

In Figure 8, a displacement of 1  $\mu\text{m}$  represents a force of 10 N on the diaphragm. The change in capacitance with pressure is shown in Figure 9, in which thickness is 9  $\mu\text{m}$ , the radius is 4  $\mu\text{m}$  and the  $f_{\max}$  is 10 N. Because we have 20 sensors with maximum force of 200 N [6], the

force on each sensor is less than 10 N and linearity between force and sensor capacitance is guaranteed. The capacitance change for 10 N is 100 fF. The gap between moving plate and fixed plate is 15  $\mu$ m.

In Figure 9 nonlinearity between force and capacitance can be seen.

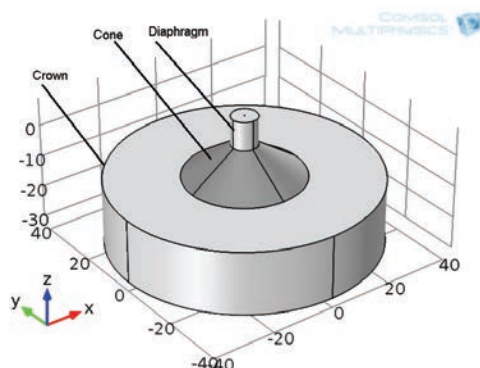


**Figure 7.** A schematic of final design. The moving plate is not shown for clarity.

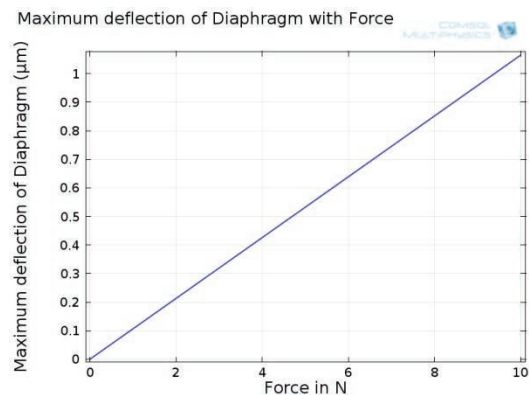


**Figure 8.** By increasing the pressure, the displacement of the moving plate increases linearly. – Graph is generated by COMSOL

By scaling the design and using some other geometries we can adjust the  $f_{max}$  and the sensitivity.

Capacitor plates consist of highly doped biocompatible polysilicon wafers..

### 3. Design of Wireless Battery-Less Power Source

Transmitting RF power from an external source to an implanted system is based on an

inductively coupled electromagnetic link. This method is widely used in biomedical devices. The movement of the tooth is limited so the orientation and distance will not change too much resulting in an almost fixed coupling(See Figure 11).

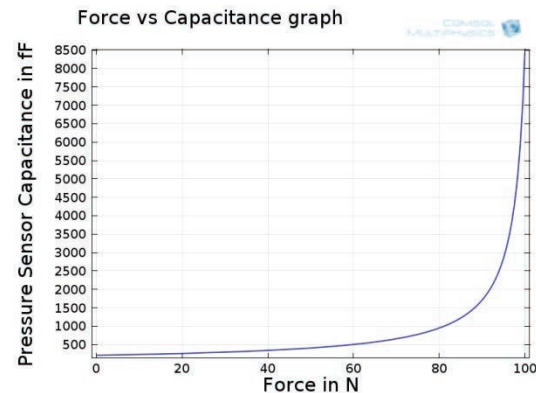


**Figure 9.** The relationship between force and capacitance change in the sensor. Graph generated by COMSOL

When we increase the number of sensors and limit the force on each sensor to 10 N the linearity can be achieved as shown in Figure 10.

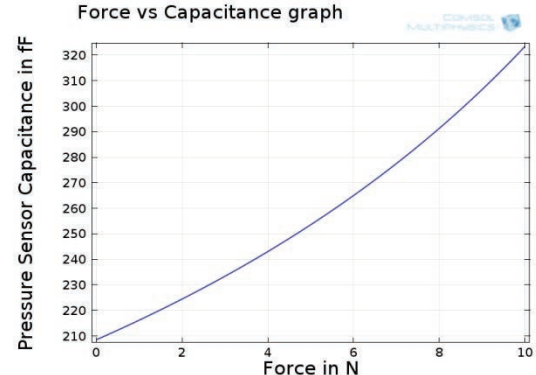


**Figure 10.** The relationship between force and capacitance change in sensor when the force is limited to 10 N. Graph generated by COMSOL

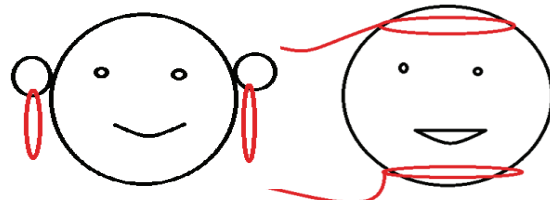


**Figure 11.** The transmitter coil/ antenna is shown as earring or necklace

Figure 12 shows a linear mode of RF powering.

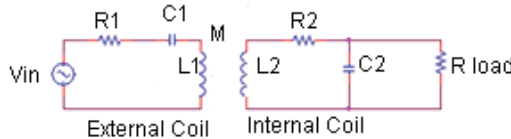


**Figure 12.** Schematic showing coupling coils used to energize the RFID as a wireless battery-less power source

Both  $L_1$  and  $L_2$  are tuned at the same frequency by capacitors  $C_1$  and  $C_2$ .

The voltage gain is given by:

$$A_v = \frac{V_{out}}{V_{in}} = \frac{\omega_0^2 M L_2}{R_1 R_2 + \frac{R_1 (\omega_0 L_2)^2}{R_{Load}} + (\omega_0 M)^2}$$

The internal coil is designed to be 5 mm in diameter (we have 10x10 mm inside the reconstruction). The external coil is designed to work 15 cm to 25 cm away from internal coil. That working distance can easily be achieved by (Figure 11) use of necklaces or earings.

Experiments have shown that AC power coupling efficiency of 0.078% can be achieved at 4 MHz with a 20 turn internal coil and a 4 turn external coil.

$$L_1 = 13.2 \mu H, L_2 = 2.6 \mu H, R_1 = 7.0 \Omega, \\ R_2 = 2.53 \Omega, \quad 0.0008 < k < 0.0034$$

An RFID chip, Figure 13, is used with the above mentioned coil replacing with the original antenna [5].

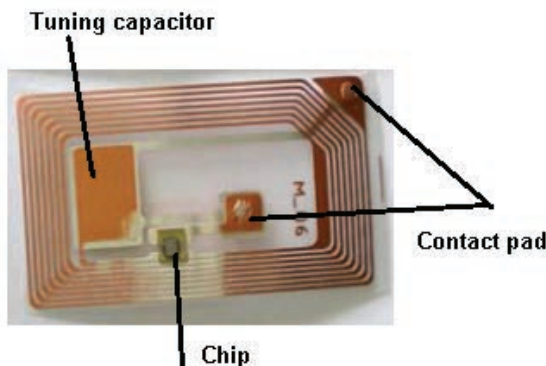


**Figure 13.** A commercial RFID Tag

The first approach: the capacitive sensor is added parallel to tuning capacitor (Figure 14) [7].

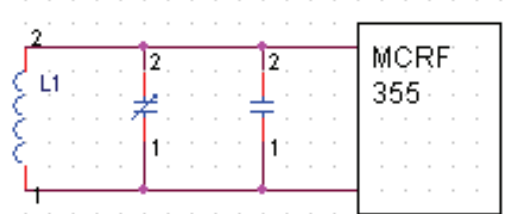


**Figure 14.** Capacitive sensor added in parallel to tuning capacitor

The capacitance change in the capacitive sensor is much smaller than the tuning capacitor of the commercial RFID. The RFID can be energized at  $f_r = \frac{1}{2\pi\sqrt{LC}}$ , where  $L$  is added coil inductance and  $C$  is the tuning capacitor. Capacitive sensor causes a deviation in return frequency of the RFID. This frequency change is retrieved by a digital signal processing techniques at the receiver/ monitoring system.

The frequency change with the force is shown in Figure 15. In that graph  $L_1$  is  $2 \mu H$  and the tuning capacitance is  $60 \text{ pF}$ .

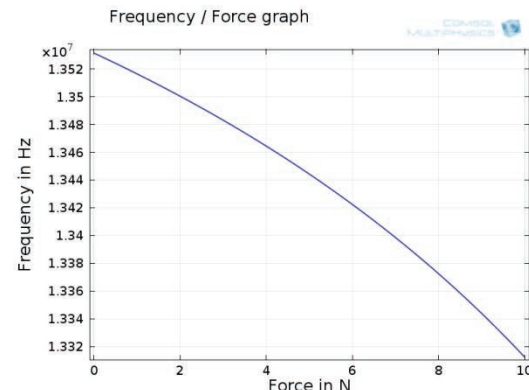


**Figure 15.** The relationship between force and resonance frequency. With smaller range of force we can achieve a linear relationship between force and resonance frequency. Graph generated by COMSOL

For MCRF355 from Texas Instrument, at a resonance frequency of 13.56MHz and a bandwidth of 140 kHz (70 kHz is its data rate), the  $Q_{max} = f_r/B$  is 96.8. It's Q is 40 in practice. Thus, the real bandwidth would be 440 kHz. This means that frequency changes, caused by our capacitive sensor, are acceptable if the

frequency change is less than 440 kHz. For  $C_{sensor}$  equal to 0.5 pF,  $C_{RFID}$  is equal to 12 pF and  $L_{coil}$  is equal to 13.5  $\mu$ H, and  $f_{max}=13.7$  MHz and  $f_{min}=13.37$ MHz, where  $f_{max}-f_{min}$  is 330 kHz. By energizing RFID in a fixed frequency of 13.56 MHz, the RFID would turn on. The matching impedance change shows less than 5% change and confirms that RFID turns on. The solid line in Figure 16 shows the impedance of tank circuit ( shown in Figure 11) when the capacitance of the pressure sensor has reached its maximum and the dotted line shows the impedance of the tank circuit when the capacitance of the pressure sensor is at its minimum.

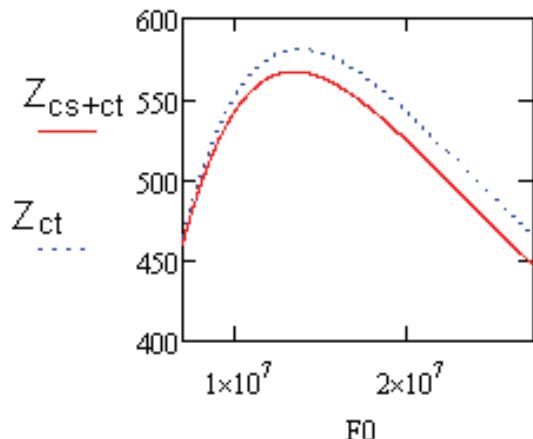


**Figure 16.** The impedance change between  $f_{max}$  and  $f_{min}$  is less than 5% (20/550)- (graph generated by MATHCAD). The solid line shows the impedance of the LC tank ( shown in Figure 9) when the capacitance of the pressure sensor is at maximum and the dotted line shows the impedance of the LC tank when the capacitance of the pressure sensor is at its minimum.

In this case:  $C_T = \frac{C_1 C_2}{C_1 + C_2}$ ,  $f_{tuned} = \frac{1}{2\pi\sqrt{LC}}$  and

$$f_{detuned} = \frac{1}{2\pi\sqrt{LC_1}}$$

As a consequence, we have a frequency change with a capacitance change in the sensor. The range can be adjusted by putting a parallel capacitor of 10 pF compared with 1 pF in capacitive sensor.

## 5. Conclusions

Capacitive pressure sensor with low temperature dependence, miniature size, low power consumption and suitable dynamic pressure range was designed and simulated. The simulations by COMSOL verify the assumptions and calculations and confirm that the model should work properly. Also, by using a RFID chip with small coil as an antenna makes the whole design small enough so it can be placed inside a pontic. Also, by adjusting the energizing frequency to comply with the capacitive sensor change, the best result can be generated.

## 6. References

1. J.O. Dennis, M.S.B. Mat Sihat,, A. Yousif Ahmed and Farooq Ahmad " Piezoresistive Pressure Sensor Design, Simulation and Modification using Coventor Ware Software" *Journal of Applied Sciences*, **8**, pp. 1426-1430, (2011).
2. Stephen D. Senturia " Microsystem Design" Kluwer Academic Publisher, (2001).
3. 2. Y. Zhang, R. Howver, B. Gogoi and N. Yazdi "A High-Sensitive Ultra-Thin MEMS Capacitive Pressure Sensor" *International Conference on Solid State Sensors and Actuators-Transducers*, pp. 112-115, June (2011).
4. Peng Cong, Wen H. Ko, and Darrin J. Young, "Wireless Batteryless Implantable Blood Pressure Monitoring Microsystem for Small Laboratory Animals" PH.D. Dissertation, Case Western University *IEEE Sensors journal*, **10**, pp. 243-254 (2010)
5. Albert Lozano-Nieto, "Educating students in the new wireless technologies: Educational experiences in RFID systems," *the Technology Interface Journal*, **10**, No. 3 Spring (2010).
6. Kaoru Kohyama and Tomoko Saki S, "Intraoral Pressure Measurement during Mastication of Kelp," *Food Sci. Technol. Res.*, **7**(1), pp. 17–21 (2001).
7. Youbok Lee, "Antenna Circuit Design for RFID Applications," AN710, *Microchip Technology Inc.*, (2003)